

matic change, the present cause is the greater magnitude and frequency of peak stream flow in response to impervious urban surfaces. This study joins a growing literature on the role of sediment storage in general; and, in particular, shows that sediment storage loss from stream channel erosion over varied geographic regions can be a major source of sediment yield (13). In such cases, sediment yield per unit area can actually increase with basin area rather than decrease, as is commonly perceived.

Suspended sediment measuring stations in sand-bed channels can underestimate total sediment loads (14), and this may be the case for San Diego Creek. If substantial, the additional sediment yield could relegate channel erosion to a somewhat smaller proportion of total sediment yield but probably no less than half. Erosion of earthen channels will remain a substantial source of sediment yield from urban stream systems until proper ameliorative measures are taken.

#### REFERENCES AND NOTES

1. S. Trimble, in preparation.
2. M. Wolman, *Geogr. Ann.* **49A**, 385 (1967).
3. M. Wolman and A. Schick, *Water Resour. Res.* **3**, 451 (1967); L. Leopold, *U.S. Geol. Surv. Circ.* **554** (1968); *Geol. Soc. Am. Bull.* **84**, 1845 (1972); W. Graf, *ibid.* **11**, 690 (1975); G. Hollis and J. Luckett, *J. Hydrol.* **30**, 351 (1976); W. Graf, *Water Resour. Res.* **13**, 459 (1977); C. Arnold, P. Boison, P. Patton, *J. Geol.* **90**, 155 (1982); H. Chang and D. Stow, *J. Hydrol.* **99**, 201 (1988); F. Ebisemiju, *Appl. Geogr.* **9**, 273 (1989); R. Neller, *Environ. Geol. Water Sci.* **14**, 167 (1989); C. Roberts, in *Floods: Hydrological, Sedimentological, and Geomorphological Implications*, K. Beven and P. Carling, Eds. (Wiley, Chichester, UK, 1989), pp. 57–82; D. Booth, *Water Resour. Bull.* **26**, 407 (1990); K. Gregory, R. Davis, P. Downs, *Appl. Geogr.* **12**, 299 (1992); F. Odermertho, *Prof. Geogr.* **44**, 332 (1992).
4. T. Hammer, *Water Resour. Res.* **8**, 1530 (1972).
5. National Research Council, *Watershed Research in the U.S. Geological Survey* (National Academy Press, Washington, DC, 1997).
6. R. Cooke, D. Brunnsden, J. Doornkamp, D. Jones, *Urban Geomorphology in Drylands* (Oxford, UK, 1982); W. L. Graf, *Fluvial Processes in Dryland Rivers* (Springer-Verlag, Berlin, 1988); M. Newson, *Land, Water and Development* (Routledge, London, 1992).
7. Boyle Engineering Corporation, *Hydrologic Analysis, Newport Bay Watershed, San Diego Creek Comprehensive Stormwater Sedimentation Control Plan, Part II, Task II-A*, Technical Memorandum (San Diego, CA, 1981).
8. S. Trimble, *Geomorphic Analysis, Newport Bay Watershed, San Diego Creek Comprehensive Stormwater Sedimentation Control Plan, Part II, Task II-B*, Technical Memorandum (Boyle Engineering, San Diego, CA, 1981).
9. B. Hoag, thesis, University of California, Los Angeles (1983).
10. The 1983–85 annual reports are on file at the Environmental Studies Section, Orange County Environmental Management Agency (OCEMA), Anaheim, CA. The 1986–93 reports are included in the Annual Reports, San Diego Creek Sediment Monitoring Program (OCEMA, Santa Ana, CA).
11. S. Trimble, in *San Diego Creek Sediment Monitoring Program Annual Report, 1992–1993* (OCEMA, Santa Ana, CA, 1994), appendix B. Available at [www.geog.ucla.edu/faculty/trimble.html](http://www.geog.ucla.edu/faculty/trimble.html).
12. R. Cooke and R. Reeves, *Arroyos and Environmental Change in the American Southwest* (Clarendon

Press, Oxford, UK, 1977).

13. S. W. Trimble, *Science* **188**, 1207 (1975); S. A. Schumm, M. P. Mosley, G. L. Zimpfer, *ibid.* **191**, 871 (1976); S. W. Trimble, *ibid.*, p. 871; W. Dietrich and T. Dunne, *Zeits. Geomorphol. Suppl.* **29**, 191 (1978); H. Kelsey, *Geol. Soc. Am. Bull.* **91**, 190 (1980); S. W. Trimble, *Science* **214**, 181 (1981); F. Swanson, F. Janda, T. Dunne, D. Swanston, Eds., *Sediment Budgets and Routing in Forested Drainage Basins* (U.S. Department of Agriculture, Forest Service General Technical Report PNW141, 1982); R. Meade, *J. Geol.* **90**, 235 (1982); P. Patton and P. Boison, *Geol. Soc. Am. Bull.* **97**, 369 (1986); J. Phillips, *Am. J. Sci.* **287**, 780 (1987); M. Church and O. Slaymaker, *Nature* **337**, 352 (1989); J. Knox, *Int. Assoc. Hydrol. Sci. Pub.* **184**, 157 (1989); P. Ashmore, *Prog. Phys. Geogr.* **17**, 190 (1993); A. Schick and J. LeKach, *Phys. Geogr.* **14**, 225 (1993); O. Slaymaker, *ibid.*, p. 305; S. Trimble, in *Changing River Channels*, A. Gur-
14. W. Emmett, R. Myrick, R. Meade, *U.S. Geol. Surv. Open-File Rep.* **80-1189** (1980); W. Rose, *U.S. Geol. Surv. Water Resour. Inv. Rep.* **90-4124** (1992); K. Fowler and J. Wilson, *U.S. Geol. Surv. Water Resour. Inv. Rep.* **95-4135** (1997).
15. I thank the U.S. Geological Survey, Water Resources Division; the Orange County Environmental Management Agency; the California Water Resources Council; and the University of California, Los Angeles (UCLA), Faculty Senate for funding this study. This paper was improved by comments from R. Ambrose, W. W. Emmett, W. L. Graf, J. Harvey, R. Mattoni, A. Mendel, L. Smith, and M. G. Wolman. I also thank the many UCLA students who assisted me in the field research.

24 June 1997; accepted 16 October 1997

## Adatom Pairing Structures for Ge on Si(100): The Initial Stage of Island Formation

X. R. Qin and M. G. Lagally\*

With the use of scanning tunneling microscopy, it is shown that germanium atoms adsorbed on the (100) surface of silicon near room temperature form chainlike structures that are tilted from the substrate dimer bond direction and that consist of two-atom units arranged in adjoining substrate troughs. These units are distinctly different from surface dimers. They may provide the link missing in our understanding of the elementary processes in epitaxial film growth: the step between monomer adsorption and the initial formation of two-dimensional growth islands.

Because of its importance in microelectronics and its unique properties, the (100) surface of silicon has been extensively investigated. Driven by the capability of the scanning tunneling microscope (STM) to view this surface easily with atomic resolution, Si(100) in particular has been used as a model to understand the atomistic mechanisms of film growth (1). For both Si and Ge deposition, early stages of growth at low temperatures produce many stable adsorbed dimers (called ad-dimers), that is, two atoms that clearly remain bound to each other for extended times, as well as rows of many such ad-dimers (called islands) (2, 3). Following classical nucleation theory, in which growth occurs by the addition of atoms to a "critical nucleus" (4), it was postulated that Si or Ge monomers deposited on the Si(100) surface diffuse to form ad-dimers and that the ad-dimer is the stable nucleus from which all subsequent larger growth structures (such as the ad-dimer row islands) evolve by addition of further monomers (2). Intermediate structures ("diluted-dimer islands"), in which alternate ad-

dimers in ad-dimer row islands are missing (5) and in which the remaining ad-dimers are rotated (6), are thought to arise from individual ad-dimers and to represent an early growth stage (5, 7). Yet this evolution from single ad-dimer to any of the larger structures has not been observable, despite the intrinsic ability of the STM to do so. Hence, a critical element of understanding is missing: the atomistic pathway from the initial adsorbed monomers to the existence of stable ad-dimer row islands. The role of the ad-dimer as the essential element in this pathway has so far not been questioned.

In this report, we describe high-resolution STM observations of structures formed during the initial growth of Ge on Si(100)(2 × 1) near room temperature, in which the Ge atoms exist as two-atom units that are distinctly different electronically and structurally from any dimer in or on the surface. We show that they provide a physically reasonable link between monomer adsorption and diluted-dimer island formation. We suggest that, at least at low temperatures, ad-dimers are not part of the nucleation-growth pathway.

The experiments were performed on Si(100) with a high-quality 2 × 1 surface and a defect density of <0.5%, in an STM outfitted with an evaporation source from

University of Wisconsin-Madison, Madison, WI 53706, USA.

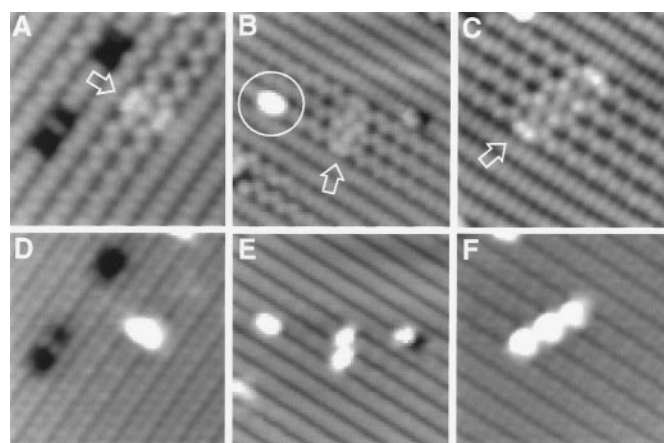
\*To whom correspondence should be addressed at [lagally@engr.wisc.edu](mailto:lagally@engr.wisc.edu)

which Ge was deposited to coverages of typically  $\sim 0.01$  monolayer (ML), while the substrate temperature was maintained below 330 K. These conditions produce chainlike structures on the surface (Fig. 1), with three common features: (i) They form across the substrate dimer rows and are terminated by two adjacent dimers buckled in the same direction, (ii) they induce locally pinned  $c(2 \times 4)$  buckling in the substrate dimer rows, and (iii) they extend along a direction tilted  $26.6^\circ$  to that of the substrate dimer bond. Such structures have recently also been observed by others (8, 9), but with a range of measurements insufficient to demonstrate their unique character.

Filled-state images are shown in Fig. 1, A, B, and C. In corresponding empty-state images (Fig. 1, D, E, and F), the chain structures appear as bright oval or round protrusions symmetrically located in the troughs between the substrate dimers. Such a symmetrical appearance implies that each building unit of the chain structure is formed from two atoms because monomer adsorption would result in an asymmetrical intensity in the trough (10). Bias-dependence imaging of the surface (Fig. 2) demonstrates additional properties of the chain units. The oval shape of each unit in the chain in the empty-state images (Figs. 2, B and C) changes noticeably with sample bias, but the longer axis (the axis of the two atoms in a chain unit) remains perpendicular to the substrate dimer rows, independent of bias.

We now demonstrate that the two atoms in each unit of the chain structure (hereafter referred to as adatom pairs) do not behave like ad-dimers. Ad-dimers are found in several configurations on the surface, individually on top of substrate dimer rows (circle in Fig. 1B), in a diluted-dimer island (rectangles in Fig. 2), and as part of a three-atom cluster (arrows in Fig. 2). In all cases, they appear much brighter in filled-state images than do adatom pairs (compare ellipse in Fig. 2A). Ad-dimers also do not show a clear change in brightness when the bias polarity is reversed. In contrast, the brightness of adatom pairs does change with bias reversal (Figs. 1 and 2). This dependence of the brightness on the bias polarity is similar to that of monomers adsorbed at the ends of dimer row islands (11) or the ends of diluted-dimer islands (rectangle and arrow in Fig. 2). This brightness effect is especially noteworthy in comparisons of ad-dimers in diluted-dimer islands (rectangles, Fig. 2) and adatom pairs (ellipses, Fig. 2) because both are located in the troughs between substrate dimer rows and both have their axes perpendicular to the substrate

**Fig. 1.** STM images of 0.01-ML Ge adsorbed on Si(100) ( $2 \times 1$ ). The long bands running through the diagonal of the frames are the substrate dimer rows. In the filled-state images (A to C), individual substrate dimers appear symmetric (bean shapes) or buckled (smaller zigzag protrusions along the dimer rows). Three typical Ge adatom-induced chainlike structures are shown by arrows. They were obtained with a tunneling current of 0.2 nA at  $-2$ -V sample bias relative to the STM tip. A single ad-dimer on top of a substrate dimer row is shown in the circle in (B). The appearance of the structure in (C) as a chain with three links leads to the term "chain structure." (D to F) Corresponding empty-state images of the identical regions, obtained with  $+2$ -V bias. At this bias, because of the distribution of charge on the surface, the centers of substrate dimer rows appear as darkened bands. The troughs occur halfway between, in the bright region, and can frequently be seen as a weaker dark line. The units of the chain structures reside in the troughs. Image sizes are  $60 \text{ \AA}$  by  $60 \text{ \AA}$  (A and D),  $75 \text{ \AA}$  by  $75 \text{ \AA}$  (B and E), and  $70 \text{ \AA}$  by  $70 \text{ \AA}$  (C and F).



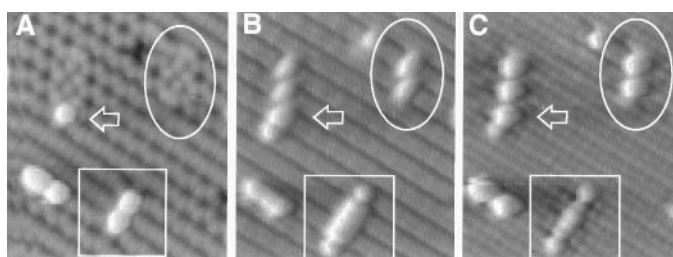
dimer rows. In addition to this radical brightness effect, which distinguishes between ad-dimers and adatom pairs, differences are observed at positive sample bias in the behavior of an adatom pair (ellipses, Fig. 2) and an ad-dimer in a diluted-dimer island (rectangles, Fig. 2). Their shapes differ at a given sample bias and vary differently with the bias (Fig. 2, B and C). All these spectroscopic indications suggest an electronic structure for the adatom pairs that differs from the dimer bond in ad-dimers and implies a structural difference.

It might be argued that the faint appearance of the adatom pairs in filled-state images is caused by their position in the chain, but this is not so (Fig. 3). The structure enclosed by the square in Fig. 3 consists of an ad-dimer (the bright protrusion) and a faint unit that behaves like an adatom pair. The shape of the latter varies with bias in the same fashion as the ada-

tom pairs (ellipses, Fig. 2), whereas the shape of the former does not vary and its brightness remains high. The structure enclosed by circles in Fig. 3 consists of two identical ad-dimers: Neither changes shape or brightness with changing bias. Clearly, an adatom pair differs from an ad-dimer, even on structurally equivalent sites.

We propose a model for the adatom pair as follows. The global adsorption energy minimum for a Ge monomer on Si(100) is calculated to be at the "M" site, which is directly above a second-layer substrate atom (Fig. 4A) (10). We suggest that adatoms adsorb on the two nearest opposing M sites of neighboring dimer rows (Fig. 4B). The bias-polarity dependence of brightness, similar to that of monomers, implies that the two adatoms in an adatom pair have an electronic structure similar to that of monomers. The driving force pairing the monomers into

**Fig. 2.** Images of three types of early-stage structures formed by Ge on Si(100), viewed at different biases: (A)  $-2$  V, (B)  $+2$  V, and (C)  $+1.2$  V. Ellipses indicate a chain structure spanning three substrate dimer rows. Rectangles indicate a diluted-dimer island with a monomer at each end. Diluted-dimer islands, in which ad-dimers arrange themselves end to end in troughs, coexist with the chain structures. A monomer is often found at the ends of such islands. It appears as a localized dark shadow in the filled-state image (A) and as a bright protrusion in the empty-state images (B and C). Arrows indicate an ad-dimer in a trough with an attached monomer, at the end of a chain structure. The bias dependencies are discussed in the text. Image size is  $85 \text{ \AA}$  by  $90 \text{ \AA}$ .



the nearest opposing M sites can be understood in terms of strain-mediated substrate dimer buckling as a result of Ge adsorption. Recent theoretical results have shown that a single Ge atom adsorbed at an M site induces strong in-phase buckling in the two substrate dimers nearest to the Ge adatom on the adjacent dimer row (Fig. 4A) (10). This pinned buckling would effectively leave a “hollow” at the M site that lies between these lowered Si atoms [in-phase substrate dimer buckling is one of three common features observed for chain structures (Fig. 1)]. Ab initio calculations (12) for Si(100) show that the binding of a Si monomer at the “down” side of a buckled substrate dimer is stronger than that at the “up” side of the substrate dimer. We expect that this result can also be applied to Ge atom adsorption. Combining the above two arguments leads to an energetic advantage, after an M-site adsorption of Ge, for the subsequent Ge adsorption to occur on the directly opposite M site, producing the pairing tendency. Direct adatom-adatom interaction is not required, but it also cannot be completely excluded. It is possible that the two atoms are in a bound state somewhere between monomers paired only by a substrate strain-mediated interaction and an ordinary ad-dimer. Their similarity in behavior to monomers suggests that a direct interaction is weak. In any case, individual adatom pairs, larger chain structures, and mixed structures (squares, Fig. 3) remain stable at room temperature for at least 8 hours, suggesting a substantial kinetic barrier to keep the adatom pair from forming a regular ad-dimer.

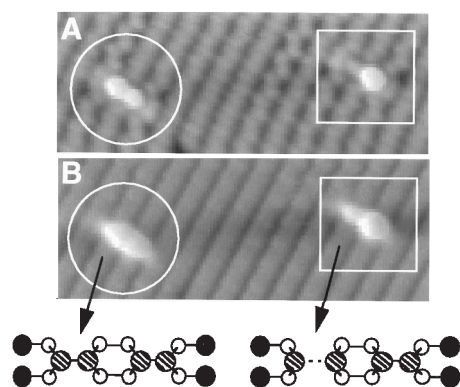


**Fig. 3.** Comparison at different biases [(A)  $-2$  V and (B)  $+2$  V] of images of structures containing ad-dimers only and a mixture of ad-dimer and adatom pair. Squares indicate a mixed structure of an adatom pair and an ad-dimer. Circles indicate a diluted-dimer island consisting of two ad-dimers. The behavior of each part of the mixed structure is consistent with that of the corresponding pure structure. Image size is  $110$  Å by  $45$  Å.

We believe that this adatom pairing is the actual initial step in the formation of a growth structure. Formation of the extended chains may be rationalized as follows. An adatom pair (Fig. 4B) breaks  $\pi$  bonds on the substrate dimers involved (13), creating four dangling bonds. These most reactive dangling bond sites provide a nucleation center for further attachment of adatoms. If one simply counts dangling bonds, the M sites on the axis of the initial adatom pair would seem to be the most favorable adsorption sites. However, because these dangling bonds are located at “up” sides of the two in-phase buckled substrate dimers, the binding of a monomer there could easily be weaker than at the M sites shifted one dimer along the dimer row. The second adatom pair then forms in the adjoining trough offset from the first pair. Obviously, the third pair has

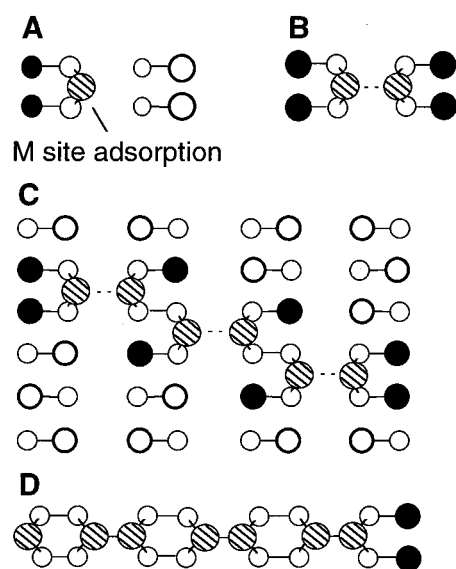


**Fig. 4.** Schematic models for early structures formed by Ge on Si(100), viewed from the top. Hatched circles, Ge adatoms; open circles, substrate Si atoms; solid circles, substrate Si atoms with dangling bonds released from the  $\pi$  bonding. Higher atoms are represented by larger circles. (A) Minimum-adsorption-energy “M” site. The adsorbed monomer breaks two  $\pi$  bonds on the adjacent dimers, creating two dangling bonds on the solid atoms. The adsorption at the M site causes in-phase dimer buckling on the neighboring dimer row, with the closer atoms moving lower. (B) The proposed model for a chain unit, the adatom pair on M sites. The dashed line indicates that the interaction between the adatoms is different from that in a conventional dimer bond. Four dangling bonds exist on the up-buckled (solid) atoms. The distance between the two opposing M sites is  $3.84$  Å (10). (C) A three-unit chain structure. The dangling bonds on the solid atoms define the unique image of the chain structures (for example, Fig. 1C). (D) A diluted-dimer island with three ad-dimers and a monomer at the left end. The dimer bond length is  $\sim 2.35$  Å (7).

two choices relative to the second pair, resulting in either line- or zigzag-shaped chain structures, both of which we have observed.

Similar chain structures recently observed for Si on Si(100) (8) and Ge(100) (9) surfaces were interpreted (because of an insufficient range of bias-dependence measurements) as being constituted of ad-dimers, that is, the same as in diluted-dimer islands (5, 6), implying that the chain structure is simply an alternative to the diluted-dimer island. It has been argued that the difference in brightness was related to the two arrangements (offset compared with in one line) of the ad-dimers (8). This interpretation begs the question of how monomers form growth islands and also cannot explain our bias-dependence measurements. Our own experiments for Si on Si(100) confirm our picture, and from a careful analysis of the data we conclude that the same is true for Si on Ge(100) as well (14).

Our results allow us to establish a logical link between the adsorption of monomers and the formation of growth structures. We suggest that the chain structures formed by adatom pairs are metastable intermediates in the formation of the diluted ad-dimer rows, with a higher free energy but lower kinetic barrier for formation. These chain structures have more dangling bonds and induce a larger area of substrate dimer buckling. Indeed, experiments done at higher substrate temperatures lead to a diminishing density of the chain structures and an increasing number of the diluted-dimer islands, showing that the latter are energetically favorable. In any case, the adatom pairs described here must form first. The third arriving adatom has two choices: (i) residing at one of the laterally displaced M sites, the process favoring the formation of the chain structures described here, or (ii) residing on the kinetically less favorable “in-line” M site that is between the “up” ends of the in-phase buckled dimers, the process that would lead to the direct formation of diluted-dimer islands. For the first choice, a mechanism must exist for transforming chain structures into diluted-dimer islands. Although the pathway is not known, it must involve formation of ad-dimers from adatom pairs and realignment from the canted chains to the diluted-dimer islands. For Ge on Si(100), Si on Si(100), and Si on Ge(100), different amounts of lattice strain can affect the temperature dependence of the relative rates of these processes.

Our identification of adatoms paired across troughs between dimer rows as the initial stage (at temperatures at least as

high as 350 K) of dimer row island formation in Si(100) has intriguing consequences. Besides providing a logical pathway from adatom adsorption and diffusion to growth of islands, these chain structures and their prevalence suggest that the smallest and most obvious stable structure on the surface, the ad-dimer residing on top of the dimer rows, does not participate in a fundamental way in the growth of larger dimer row islands. If this is so, it will require reevaluation (at least on semiconductor surfaces) of the concept of a critical nucleus for growth and of the many rate equation models for diffusion and growth on this surface, which all require the size of a critical nucleus as input. We no longer appear to have, at these temperatures, a well-defined critical or stable nucleus be-

cause growth proceeds from long-lived metastable structures that may have a variety of sizes.

#### REFERENCES AND NOTES

1. For a review and an extended list of references, see Z. Zhang and M. G. Lagally, *Science* **276**, 377 (1997).
2. Y.-W. Mo and M. G. Lagally, *Surf. Sci.* **248**, 313 (1991); Y.-W. Mo, J. Kleiner, M. B. Webb, M. G. Lagally, *Phys. Rev. Lett.* **66**, 1998 (1991); *Surf. Sci.* **268**, 275 (1992).
3. R. J. Hamers, U. Köhler, J. E. Demuth, *Ultramicroscopy* **31**, 10 (1989); Y.-W. Mo, R. Kariotis, D. E. Savage, M. G. Lagally, *Surf. Sci.* **219**, L551 (1989); J. Y. Tsao, E. Chason, U. Köhler, R. J. Hamers, *Phys. Rev. B* **40**, 11951 (1989).
4. J. A. Venables, *Philos. Mag.* **27**, 697 (1973). The "critical nucleus" is defined as that structural entity for which the addition of one more atom will for the first time reduce the free energy of the entity. It can be as little as one atom. The stable nucleus is the smallest

- structural entity with a negative free energy. It can be as little as two atoms.
5. Y.-W. Mo, R. Kariotis, B. S. Swartzentruber, M. B. Webb, M. G. Lagally, *J. Vac. Sci. Technol. A* **8**, 201 (1990).
  6. P. J. Bedrossian, *Phys. Rev. Lett.* **74**, 3648 (1995).
  7. G. Brocks and P. J. Kelly, *ibid.* **76**, 2362 (1996).
  8. J. van Wingerden, A. van Dam, M. J. Haye, P. M. L. O. Scholte, F. Tuinstra, *Phys. Rev. B* **55**, 4723 (1997).
  9. W. Wulfhekkel, B. J. Hattink, H. J. W. Zandvliet, G. Rosenfeld, B. Poelsema, *Phys. Rev. Lett.* **79**, 2494 (1997).
  10. V. Milman *et al.*, *Phys. Rev. B* **50**, 2663 (1994).
  11. B. S. Swartzentruber, *ibid.* **55**, 1322 (1997).
  12. Q.-M. Zhang, C. Roland, P. Boguslawski, J. Bernholc, *Phys. Rev. Lett.* **75**, 101 (1995).
  13. J. A. Appelbaum, G. A. Baraff, D. R. Hamann, *Phys. Rev. B* **14**, 588 (1976).
  14. X. R. Qin and M. G. Lagally, unpublished data.
  15. We thank B. Swartzentruber for valuable advice and help. Supported by NSF (grant DMR93-04912) and by Sandia National Laboratory (grant AS-1168).

14 July 1997; accepted 14 October 1997

## Vigorous HIV-1-Specific CD4<sup>+</sup> T Cell Responses Associated with Control of Viremia

Eric S. Rosenberg, James M. Billingsley, Angela M. Caliendo, Steven L. Boswell, Paul E. Sax, Spyros A. Kalamas, Bruce D. Walker\*

Virus-specific CD4<sup>+</sup> T helper lymphocytes are critical to the maintenance of effective immunity in a number of chronic viral infections, but are characteristically undetectable in chronic human immunodeficiency virus-type 1 (HIV-1) infection. In individuals who control viremia in the absence of antiviral therapy, polyclonal, persistent, and vigorous HIV-1-specific CD4<sup>+</sup> T cell proliferative responses were present, resulting in the elaboration of interferon- $\gamma$  and antiviral  $\beta$  chemokines. In persons with chronic infection, HIV-1-specific proliferative responses to p24 were inversely related to viral load. Strong HIV-1-specific proliferative responses were also detected following treatment of acutely infected persons with potent antiviral therapy. The HIV-1-specific helper cells are likely to be important in immunotherapeutic interventions and vaccine development.

Infection with HIV-1 is characterized by a quantitative decline in the number of CD4<sup>+</sup> lymphocytes and a qualitative impairment of their function (1). Immunological abnormalities in T helper cell function occur early, during the asymptomatic phase of infection and before the loss in CD4<sup>+</sup> cell number (2). Loss of T cell function in vitro predicts progression to acquired immunodeficiency syn-

drome (AIDS) and a decrease in survival time (3). In addition to these general defects in lymphocyte function, infection typically fails to induce detectable HIV-1-specific proliferative responses (4). It is thought that CD4<sup>+</sup> helper cell responses play a key role in maintaining effective immunity in murine models of chronic viral infections (5). In HIV-1 infection, the lack of virus-specific proliferative responses is the most dramatic defect in the repertoire of the immune system. When such responses have been observed, they are typically weak, with stimulation indices (SIs) rarely greater than 5 (6).

Recently, a subset of HIV-1-infected persons who appear to successfully control virus replication in the absence of antiretroviral therapy has been identified. Despite infections of up to 18 or more years, these individuals maintain normal CD4<sup>+</sup> T cell counts, low to undetectable viral loads, and

have no evidence of HIV-1-related disease manifestations (7). The persistence of vigorous cytolytic T lymphocyte (CTL) and humoral immune responses in some of these individuals suggests that the host immune response may be effectively containing viral replication (8). Given the demonstrated importance of virus-specific CD4<sup>+</sup> T helper cell responses in other chronic viral infections, we examined individuals with long-term nonprogressive infection for evidence of such responses directed against HIV-1.

Initial studies were performed in an HIV-1-infected hemophiliac (subject 161-J) with 18 years of documented seropositivity, a normal CD4<sup>+</sup> T cell count, and a viral load of <400 RNA molecules per milliliter of plasma, who had never been treated with antiretroviral agents. Consistent with previous studies (9), an extremely vigorous CTL memory response was detected, with more than 1 HIV-1-specific CTL per 200 peripheral blood mononuclear cells (PBMC) (10). Freshly isolated PBMC from this subject were exposed to whole soluble HIV-1 p24 and gp160 protein, resulting in vigorous virus-specific lymphocyte proliferation (Fig. 1A). Nearly identical results were obtained with HIV-1 antigens derived from baculovirus, yeast, and Chinese hamster ovary (CHO) cells, whereas control antigens derived from the same sources elicited no responses. The PBMC stimulated with p24 resulted in the most vigorous lymphocyte proliferation, with SI > 200 to baculovirus- and CHO-derived antigens. Envelope protein gp160 elicited a less intense but significant lymphocyte proliferative response to baculovirus- and yeast-derived antigen. The responses were mediated by the CD4<sup>+</sup> T lymphocyte subset, as demonstrated by loss of activity with depletion of CD4<sup>+</sup> cells (Fig. 1B). These virus-specific proliferative responses were highly repro-

E. S. Rosenberg, J. M. Billingsley, S. A. Kalamas, B. D. Walker, Partners AIDS Research Center and Infectious Disease Unit, Massachusetts General Hospital, and Harvard Medical School, Boston, MA 02114, USA.

A. M. Caliendo, Partners AIDS Research Center and Department of Pathology, Massachusetts General Hospital and Harvard Medical School, Boston, MA 02114, USA.

S. L. Boswell, Fenway Community Health Center, Boston, MA 02115, USA.

P. E. Sax, Partners AIDS Research Center and Division of Infectious Diseases, Brigham and Women's Hospital, and Harvard Medical School, Boston, MA 02115, USA.

\*To whom correspondence should be addressed. E-mail: bwalker@helix.mgh.harvard.edu